

Opportunities for Low-Voltage TEM/STEM.

R.F. Egerton

¹ Physics Department, University of Alberta, Edmonton, Canada T6G 2E1.

The main effect of reducing the TEM accelerating voltage V_0 is to increase the fraction of electrons that are scattered elastically and inelastically. As this fraction approaches 1, plural scattering becomes excessive and is generally deleterious in TEM images and energy-loss spectra. Therefore low- V_0 TEM is attractive only for very thin specimens [1]. Fortunately there are nanotechnology samples that fulfill this requirement, such as graphene and carbon nanotubes. For such a specimen, the increased elastic-scattering power at low V_0 increases the image contrast (in bright-field imaging) or the signal (for dark-field STEM). If the specimen is electrically conducting, the predominant mechanism of radiation damage is likely to be knock-on displacement, which can often be minimized or even eliminated by using an accelerating voltage below some threshold value.

Unfortunately, reducing V_0 increases the electron wavelength λ and increases the angular spread α that must be focused by the objective lens, for a given diffraction-limited resolution: $d_d = 0.6\lambda/\alpha$. If V_0 is reduced below 40 kV, atomic resolution requires correction of both spherical and chromatic aberration, as illustrated in Table 1. It is tempting to imagine a 10 – 30kV STEM for nanotechnology specimens, similar to that used by Crewe *et al* [2], but with aberration correction. If equipped with a high-resolution monochromator, such an instrument could perform vibrational-mode EELS [3] with a spatial resolution determined by delocalization and radiation damage [4]. If provided with ultrahigh vacuum (UHV) and specimen cleaning devices, Auger spectroscopy and atomic-scale secondary-electron imaging [5] might also be possible.

For beam-sensitive materials that damage by radiolysis, there is no useful accelerating-voltage threshold and the only way to minimize radiation damage is to defocus the incident electron beam and record a signal from a large area of specimen. This of course defeats the usual goal of microscopy, which is to obtain good spatial resolution. Although both the (elastic or inelastic) signal and radiolysis damage are inversely proportional to accelerating voltage, it is misleading to say that the signal/damage ratio is independent of V_0 : factors such as specimen thickness and imaging mode should be taken into account. The dose-limited spatial resolution is $\text{DLR} \sim D^{1/2}/C$ where C = image-contrast ratio, D = tolerable dose and \sim means “proportional to”. $D \sim V_0$ for radiolysis damage, while $C \sim t/V_0$ for bright-field scattering contrast and a small sample thickness t , giving $\text{DLR} \sim V_0^{1/2}/t$. Therefore low V_0 is advantageous for very thin specimens, although $\text{DLR} > 1$ nm for typical D ; see Fig. 1a. With increasing thickness, the resolution improves until plural scattering predominates, shown by the upward curvatures in Fig. 1a. For phase contrast, $C \sim t/V_0^{1/2}$ at small t , making DLR independent of accelerating voltage [1].

Electrostatic charging is a further problem with poorly conducting thin specimens, which charge positively due to the emission of secondary and Auger electrons. In some materials, the emission current is compensated by a conduction current when the positive potential reaches some modest potential; see Fig. 1b. However, this voltage may be sufficient to cause dielectric breakdown (due to the local electric field) or even a “Coulomb explosion”, which in practice means the emission of positive ions and hole drilling in oxides [6,7]. In more insulating specimens, the potential may be many thousands of volts, sufficient to deflect the incident beam or to interfere with electron focusing. These effects are likely to

be more troublesome at low accelerating voltage because the primary electrons are then more easily deflected and because the secondary-electron yield increases with decreasing V_0 [8,10].

References:

[1] RF Egerton, Ultramicroscopy **145** (2014), p. 85.
 [2] AV Crewe *et al*, J. Appl. Phys. **39** (1968) p. 5861.
 [3] OL Krivanek *et al*, Nature **514** (2014), p. 209.
 [4] RF Egerton, Microsc. Microanal. **20** (2014), p. 658.
 [5] H Inada *et al*, Ultramicroscopy **111** (2011), p. 865.
 [6] SD Berger *et al*, Phil. Mag. B **55** (1987), p. 341.
 [7] J Cazaux, Ultramicroscopy **60** (1995), p. 411.
 [8] L Reimer, "Scanning Electron Microscopy", (Springer, Berlin) p.154.
 [9] FJ Pijper and P Kruit, Phys. Rev. B **44** (1991), p. 9192.
 [10] The author gratefully acknowledges funding from the Natural Sciences and Engineering Research Council of Canada, and encouragement from his colleagues Ute Kaiser, David Bell and Jimmy Liu.

kinetic energy $E_0 = eV_0$	α (mrad)	d_s (nm) = $0.5 C_s \alpha^3$	d_c (nm) = $0.5 C_c \alpha (\Delta E/E_0)$
30 keV	4.2	0.074	0.14
10 keV	74	400	7.4

Table 1. Angular spread α required for a diffraction limit of $d_d = 0.1$ nm, with estimates of the loss of resolution due to spherical (d_s) and chromatic (d_c) aberration, taking $C_s = C_c = 2$ mm and $\Delta E = 1$ eV.

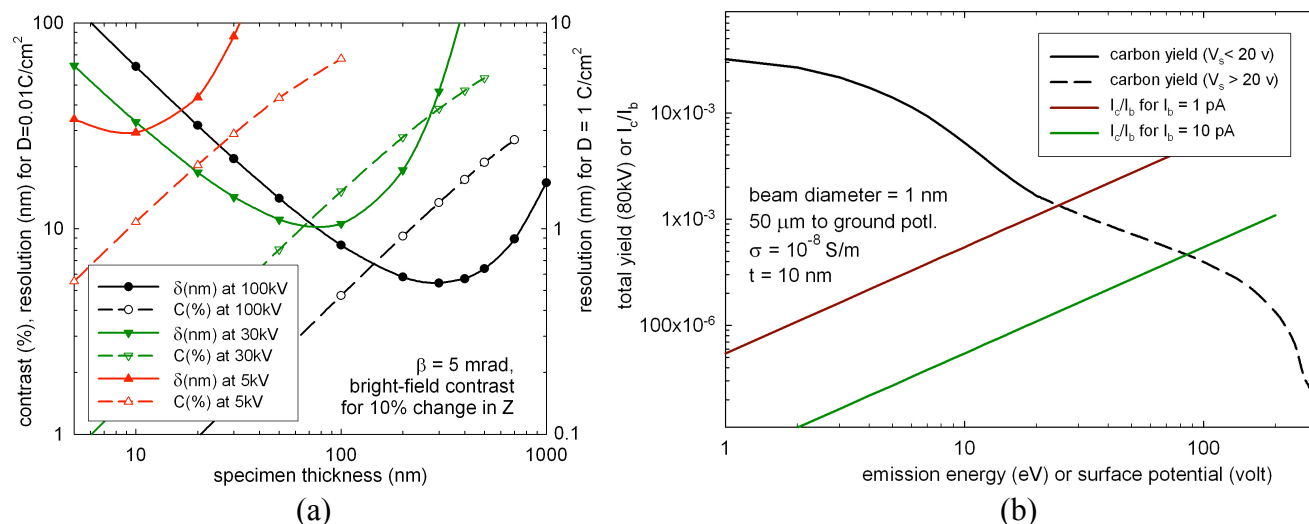


Figure 2. (a) Dose-limited resolution δ and contrast ratio C for bright-field TEM imaging (5-mrad objective aperture) at different accelerating voltages, calculated for a boundary in an amorphous specimen where the mean atomic number changes by 10%.

(b) Solid and dashed curves: total (secondary + Auger) yield for amorphous carbon as a function of surface potential [9]. Straight lines: compensating conduction current (I_c) divided by incident-beam current (I_b), for two values of I_b (1 pA and 10 pA). The intersection of these lines with the yield curve determines the value of the positive surface potential within the irradiated area.